Remote Sensing Applications: Society and Environment 37 (2025) 101425

Contents lists available at ScienceDirect

Remote Sensing Applications: Society and Environment

journal homepage: www.elsevier.com/locate/rsase

What time is the tide? The importance of tides for ocean colour applications to estuaries

Giulia Sent [a,*], Carlos Antunes [b], Evangelos Spyrakos [c], Thomas Jackson [d], Elizabeth C. Atwood [e], Ana C. Brito [a,f]

[a] MARE, Marine and Environmental Science Centre, Faculdade de Ciências, Universidade de Lisboa, 1749016, Lisboa, Portugal
[b] Universidade de Lisboa, Faculdade de Ciências, Instituto Dom Luiz, 1749016, Lisboa, Portugal
[c] University of Stirling, Earth and Planetary Observation Sciences, Stirling, FK9 4LA, UK
[d] EUMETSAT, Eumetsat Allee 1D, 64295, Darmstadt, Germany
[e] Plymouth Marine Laboratory, Prospect Place, PL1 3DH, Plymouth, UK
[f] Departamento de Biologia Vegetal, Faculdade de Ciências, Universidade de Lisboa, 1749-016, Lisboa, Portugal

ARTICLE INFO

Keywords:
Remote sensing
Transitional waters
Water quality
Turbidity
Sentinel-2

ABSTRACT

Tides can play a major role in transitional water dynamics, being the primary driver of fluctuations in water parameters. In the last decade, remote sensing methods have become a popular tool for cost-effective systematic observations, at relatively high spatial and temporal scales. However, the presence of tides introduces complexities, given that Sun-synchronous satellites will observe a different tidal condition at each overpass, effectively aliasing the daily signal. This can create non-obvious biases when using remote sensing data for monitoring tidally-dominated systems, potentially leading to misinterpretation of patterns and incorrect estimates of periodicities. In this work, we used a six-year Sentinel-2-derived turbidity dataset to evaluate the impact of tidal aliasing on the applicability of a Sun-synchronous satellite to a tidally-dominated system (Tagus estuary, Portugal). Each satellite observation was classified according to tidal phase. Results indicate that tidal processes dominated over seasonal variability, with significant differences observed between turbidity levels of different tidal phases ($p < 0.0001$). Climatology analyses also revealed significant changes between all-data and per-tidal-phase data ($p < 0.001$), highlighting the importance of classifying satellite data by tidal condition. Additionally, tidal condition labelling at each Sentinel-2 overpass revealed that not all tidal conditions are observed by a Sun-synchronous satellite, as Low tide and Floods are always observed during Spring tides and High tide and Ebbs observed under Neap tides. Spring Low tides are overrepresented compared to all other tidal conditions. This result is particularly relevant for water quality monitoring based on remote sensing data in tidally-dominated systems.

1. Introduction

Located at the transitional area between rivers and ocean, estuaries are among the most productive natural habitats in the world. The periodical mixing of freshwater and saltwater support rich biodiversity, generating ecosystems of high ecological and economic

* Corresponding author.
E-mail addresses: gsent@ciencias.ulisboa.pt (G. Sent), cmantunes@ciencias.ulisboa.pt (C. Antunes), evangelos.spyrakos@stir.ac.uk (E. Spyrakos), Thomas.Jackson@eumetsat.int (T. Jackson), liat@pml.ac.uk (E.C. Atwood), acbrito@ciencias.ulisboa.pt (A.C. Brito).

https://doi.org/10.1016/j.rsase.2024.101425
Received 15 October 2024; Received in revised form 25 November 2024; Accepted 9 December 2024
Available online 10 December 2024

value (Barbier et al., 2011; Pendleton, 2011).

While human civilizations have historically benefited from estuaries and other transitional systems, with many major settlements located nearby, the anthropogenic pressures on such habitats are increasingly growing (Kennish, 2002, Zhai et al., 2020). Hence, water monitoring has now become essential to mitigate anthropogenic impacts and preserve the health of these vital ecosystems.

The highly dynamic nature of transitional waters results in temporal changes across different timescales, from hourly variations forced by tidal currents (Nascimento et al., 2021) to seasonal and interannual fluctuations (Cereja et al., 2022), driven by astronomical and meteorological factors. They often present strong spatial and vertical gradients in water conditions (i.e. salinity, suspended sediments, and phytoplankton). These gradients can be driven by local changes in bathymetry, circulation, or the introduction and removal of dissolved and suspended constituents (Catts et al., 1985). This high spatial and temporal heterogeneity poses significant limitations on monitoring efforts, which primarily rely on costly and time-consuming field observations. Despite the generally high accuracy of in situ measurements, these are often sparse and constrained in both spatial and temporal coverage. Consequently, they are not always sufficient to provide a comprehensive understanding of these dynamic systems, particularly when information on large geographical areas or at different time-scales is required.

Satellite remote sensing methods have shown great potential for the monitoring of transitional waters, by providing information at high spatio-temporal coverage and resolution (Bierman et al., 2011). Despite the challenges in accurately interpreting the radiometric signal of transitional waters (such as water optical complexity, adjacency effect, and sun-glint), the number of successful applications of remote sensing to transitional waters is increasingly growing (Hudson et al., 2017; Tao and Hill, 2019; Wang et al., 2019; Yang et al., 2020; Sent et al., 2021; Cao and Tzortziou, 2024). In the context of water quality monitoring and coastal changes, optical sensors such as Sentinel-2-MSI, Landsat-8-OLI and Sentinel-3-OLCI mounted on Sun-synchronous satellites are often employed for monitoring these systems (Braga et al., 2020; Chen et al., 2020; Cao and Tzortziou, 2021; Oiry and Barillé, 2021; Sent et al., 2021; Masoud, 2022; Pahlevan et al., 2022; Jiang et al., 2021). Sun-synchronous satellites follow a fixed orbit that ensures they pass over a specific location at the same local solar time, to maximise the sun elevation and to minimise the sun-glint effect.

Although the interest in using remote sensing data for operational water quality monitoring is growing, when it comes to estuaries and other transitional systems, the presence of tides can add complexities that challenge the application of remote sensing data. The tidal aliasing issue has been raised in previous studies (Doxaran et al., 2009; Valente and da Silva, 2009; Eleveld et al., 2014; Normandin et al., 2019; Zhang et al., 2020; Cao and Tzortziou, 2021). However, the impact of tides on the widely employed Sentinel-2 satellites, as well as the implications for long-term data interpretation, has not yet been assessed.

Tidal waves have a 50-min delay on average at each solar day, due to the change in Moon's phase. Particularly, in semidiurnal type, this shift is due to the wave period difference in the constituents of the S2 (Solar's semidiurnal constituent with 12 h period) and M2 (Moon's semidiurnal constituent with 12 h 25 min period). Hence, in all areas dominated by tides, a Sun-synchronous satellite (in phase with S2) will observe a different tidal condition at each overpass, effectively aliasing the daily signal. Furthermore, tides are not evenly distributed throughout the day. For example, at any given location, high tide of spring tides occur roughly at the same time of the day, when the S2 and M2 are in phase (average fortnightly cycle is 14.8 days). As a result, even with a satellite that has a higher revisit time, such as Sentinel-3, certain tidal conditions will never be observed, especially in regards to the combination of spring/neap and semidiurnal cycles. This can introduce non-obvious biases when remote sensing data are used for monitoring of tide-dominated systems, leading to misinterpretation of patterns and incorrect estimates of temporal changes. While traditional in situ monitoring programs account for tidal aliasing by sampling at a similar tidal phase, remote sensing monitoring is often performed using all available images irrespective to the tidal phase at which the images were acquired. As satellite images don't contain tidal phase information, additional data should be obtained to accurately analyse remote sensing observations of tidally-dominated systems.

This paper aims to: 1) assess the capabilities of Sun-synchronous satellites for monitoring a semidiurnal tidal-dominated system under all possible tidal phases; 2) understand the magnitude of satellite-derived water quality fluctuations given by tide phases and how this affects our interpretation of time-series analysis; and 3) determine the importance of tidal phase associated with each overpass in the retrieval of water quality constituents. The implications for the use of the proposed method for operational monitoring programmes using remote sensing data are also discussed.

Using the turbidity product from the Sun-synchronous Sentinel-2 satellites for the Tagus estuary (Portugal) as an example for monitoring water quality parameters, we classified a 6-year dataset of Sentinel-2 images by tidal phase (semidiurnal) and stage (fortnightly). The objective of the tidal classification is to group satellite and/or in situ observations per tidal condition (where similar water dynamics are expected) and to remove the variability caused by tides that can potentially mask smaller-scale variability. Spatio-temporal analyses were performed on the tidally-grouped turbidity data to demonstrate that in highly dynamic systems, such as estuaries where temporal changes can occur at short-term scale (hourly), grouping the dataset by similar tidal phases can unravel smaller scale fluctuations and trends. The implications for the use of the proposed method for operational monitoring programmes using remote sensing data are also discussed.

2. Material and methods

2.1. Study area

The Tagus estuary (Fig. 1) is a tide-dominated transitional system located near Lisbon, Portugal. With an area of 320 km^2 and a mean volume of 188 km^3 (Dias and Valentim, 2013; APA, 2016), it is one of the largest estuaries in Europe and the most extensive wetland area in the Portuguese territory. In the context of the European Water Framework Directive (WFD) (European Commission, 2003), it is classified as a transitional water of typology A2 - meaning it is a well-mixed mesotidal estuary with irregular river discharge

(Bettencourt et al., 2003). The area surrounding the estuary is extensively occupied, with the western and northern margins densely urbanised, in contrast to the agricultural land use of the eastern side. Morphologically, the estuary is characterised by a deep, long, and narrow inlet that connects the Atlantic Ocean to the interior of the estuary. The system is characterised by a wide basin (15 km in the central bay) with extensive tidal flats and marshes. The intertidal areas occupy between 20 and 40% of the total estuarine area (Vaz et al., 2011),

The drainage of the Tagus estuary is mainly forced by the semi-diurnal tides, with river flow, wind, atmospheric pressure, and surface waves also playing an important role in water circulation. The main source of freshwater is the Tagus river, with a mean annual inflow between 300 and 400 $m^3 s^{-1}$ and river discharge varying mostly at seasonal time scale (Neves and dos, 2010). During a tidal cycle, the freshwater input into the estuary is only about 10% of the marine water input due to a mean tidal prism of 7.5×10^8 m^3 and mean river inflow per tidal cycle of 8.2×10^6 m^3 (Neves and dos, 2010). The Tagus estuary has asymmetric, mostly semi-diurnal tides, with an average tidal range of 2.4 m at the Lisbon tide gauge, varying from a minimum of 0.6 m in Cascais at minimum neap tides and up to 4.5 m in maximum spring tides in the upper estuary. According to Fortunato et al. (1999), the amplitude of astronomic constituents grows rapidly in the inlet channel and more steadily in the upper estuary. Due to extensive tidal flats, tides are ebb-dominated, with floods around 1 h longer than ebbs, resulting in a stronger current velocity during ebb tides (Fortunato et al., 1997, 1999; Fortunato and Oliveira, 2005). The area affected by tides reaches 80 km upstream and the maximum tidal currents are recorded at the mouth of the estuary, with values of approximately 2 m s^{-1} (Gameiro et al., 2007). M2 is the main tidal constituent with a mean tidal range of approximately 1 m (0.99 m and 1.15 m at Cascais and Lisbon tide gauges, respectively). Even though the estuary is considered well-mixed, strong stratification has been observed at high river flow events and low tidal ranges (Fortunato et al., 1997; Fortunato et al., 1999; Neves and dos, 2010).

2.2. Sentinel-2 acquisition and processing

The Sentinel-2 satellites were selected for the present work as they are frequently employed in transitional waters given their higher spatial resolution.

Water-leaving reflectance (ρw) acquired by the MSI (Multi Spectral Imager) sensor onboard the Sentinel-2 satellites were downloaded from January 2017 to December 2022 from the CERTO archive (https://engage.certo-project.org/data/). Data available on the CERTO portal are already atmospherically corrected using the Calimnos processing chain (Stelzer et al., 2020), which uses Polymer v4.15 (Steinmetz et al., 2011) atmospheric correction. Each pixel is validated by the use of a set of quality flags from the Atmospheric Correction processor (out of bounds, bright pixel masks) and IDEPIX flags (invalid, land, clouds, cirrus masks). Only dates when at least 50% of the pixels inside the polygon were flagged as valid were used for the analyses.

Based on previous validation efforts conducted in the Tagus estuary for Sentinel-2 (Sent, 2020) the semi-analytical approach proposed by Dogliotti et al. (2015) was used to estimate water turbidity. The selected algorithm is particularly suitable for estuarine

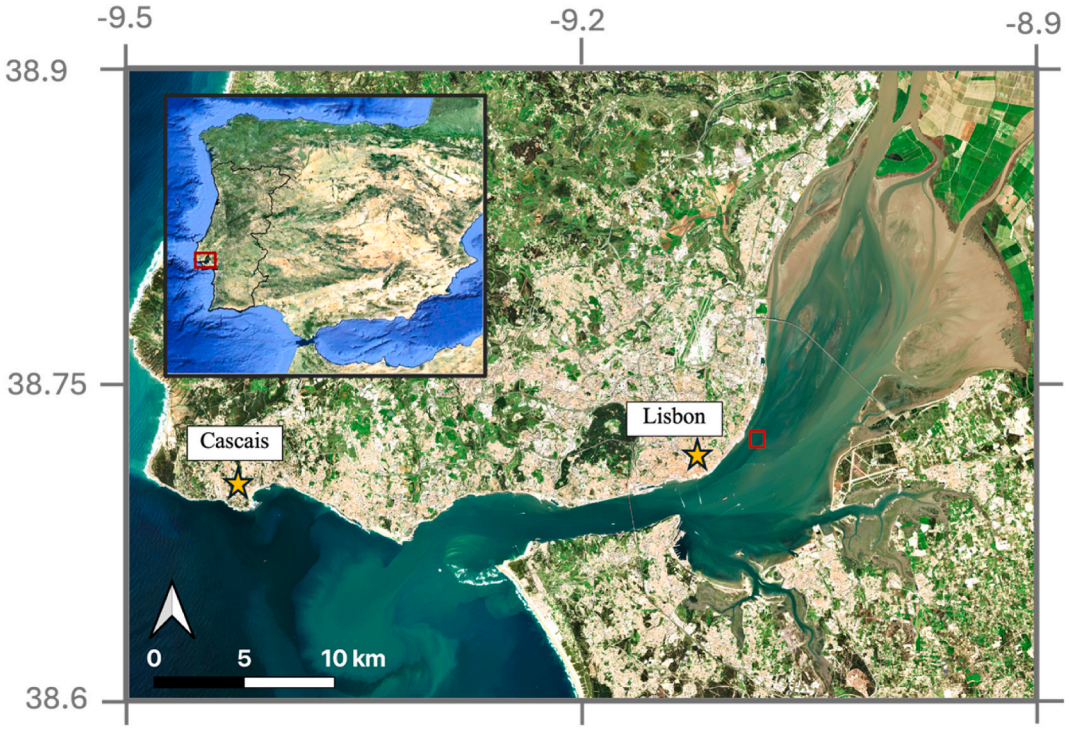

Fig. 1. The Tagus estuary with the location of the polygon (red box) used for the analysis of this work.

areas with high optical variability, as it uses a switching band method to improve the turbidity retrieval over a large range of turbidity values. Because the Tagus estuary total turbidity range is significantly lower than the original study (Dogliotti et al., 2015) and due to the unavailability of the 645 nm band for the MSI sensor, the original algorithm thresholds used for the band switch were adapted for the Tagus range and using the 665 nm band. To define the most adequate threshold values, a dataset (N = 43) of concurrent in situ turbidity and in situ ρw (665 nm, convoluted to MSI spectral band) was used. A piecewise regression was applied to identify breaking points in the linear regression between in situ turbidity and ρw665, and the values were used as thresholds to switch from the red band (665 nm) to the near-infrared band (865 nm) (Table 1).

Finally, the calibrated algorithm was applied to Sentinel-2 reflectance values and compared with an independent dataset of in situ turbidity (match-ups, N = 25) from different regions of the estuary. In situ samples were collected at the water surface and turbidity determined with a portable infrared turbidimeter (Lovibond TB210 IR). Match-ups were selected when the time difference between the satellite overpass and the in situ data collection was less than 1 h for the stations collected around the tidal peaks (weak tidal currents) and less than 30 min for the stations collected during flooding or ebbing phases. The average of 3 × 3 pixels centred on the sampling station (with >50% valid pixels) was used for the comparison.

2.3. Case study approach

A polygon of 15 × 17 pixels (resampled to 60 m) located in the middle region of the estuary (Fig. 1) was used for the analysis. The selected polygon is located in an optically deep region (no bottom reflection) at all tidal conditions and is defined by homogeneous spatial characteristics and water dynamics, making it suitable for capturing the optical variability given by different tidal conditions. Furthermore, the box is located in the proximity of the port of Lisbon, location for which the tidal harmonic model is estimated and, therefore, there is no need for time lag calculations. The choice for using a smaller polygon instead of data from the entire estuary is to prevent errors arising from potential limitations in the availability of pixels across different regions and to avoid turbidity uncertainties associated with the proximity of tidal flats and optically shallow regions. As already mentioned, the Tagus estuary is a large basin characterised by strong spatial gradients. The presence of valid pixels from different areas could introduce errors attributed to different turbidity levels resulting from spatial variability. Additionally, the per-tidal phase seasonal variability (meteorological seasons) of the turbidity product is provided at the entire estuary level through high-resolution maps.

2.4. Ancillary data

The tidal information used to classify and label each satellite overpass was obtained from the tidal prediction model of Antunes (2007) for the port of Lisbon (https://webpages.ciencias.ulisboa.pt/~cmantunes/hidrografia/hidro_mares.html).

Daily mean flow rates of river discharge at the Almourol station were obtained from SNIRH portal (https://snirh.apambiente.pt/) for the same period of Sentinel-2 data used for this study (Jan 2017–Dec 2022). Monthly means and multi-year monthly climatologies were derived from the daily means.

2.5. Tidal classification

As previously mentioned, in semidiurnal tides the 50-min delay of tidal waves each solar day is caused by the phase difference of S2 and M2 components. This is related to the month period differences of Sun (average 30.4 days) and Moon (synodic month of 29.5 days). This wave tide frequency difference is also responsible for the Spring-Neap cycle. During spring tides, the two tidal constituents are in phase and the tidal amplitude is greater (S2+M2). Neap tides occur when the S2 and M2 are in phase opposition, resulting in smaller amplitudes (S2-M2) and different water dynamics.

The objective of the tidal classification is to group satellite and/or in situ observations per tidal phase (where similar water dynamics are expected) and to remove the variability caused by tides that can potentially mask smaller-scale variability. Our proposed method was originally developed for tidal classification of a timestamp considering asymmetric semidiurnal tides, as is the case of the study area for this work. Nonetheless, it can be adopted for any type of tidal cycles (diurnal, semidiurnal, and mixed tides), as the methodology uses the time of the high and low peak to divide the tidal wave into sections of equal time. The tidal classification python code can be accessed at https://github.com/giuliasent/TidalPhaseFinder.

The schematic representation of the tidal classification is presented in Fig. 2. It consists in the division of a tidal wave into a total of 8 stages of the semi-diurnal tidal cycle. Low-Tide (LT) and High-Tide (HT) levels are set as 2 h centred at the time of the tidal peaks. The remaining time between the peaks is divided into 3 equal windows, labelled F1, F2, and F3 for Flooding tides (1 h and 31 m on average for each flooding stage) and E1, E2, E3 for Ebbing tides (1 h and 16 m on average for each ebbing stage). To classify each timestamp, we use the time and amplitudes of the tidal peaks occurring before and after each timestamp. This results in a systematic adjustment of the time window for each of the 3 phases of ebbing and the 3 phases of flooding in areas with asymmetrical tides (differing duration of

Table 1
Values range and thresholds from the original Dogliotti algorithm and adapted for the Tagus *estuary*.

	Turbidity range	thresholds for band switch
Original Dogliotti algorithm	1.8–988 FNU	$0.05 < \rho w645 < 0.07$
Tagus estuary	0.3–31.5 NTU	$0.02 < \rho w665 < 0.024$

flood and ebb), which allows to account for faster changes in water parameters due to stronger tidal currents.

The fortnightly cycle (average of 14.8 days) has been expressed in terms of tidal amplitude, with Spring tides when tidal amplitude is higher than 2.5 m and Neap tides when tidal amplitude is less than 1.5 m. An example of a monthly water level variation for the area of interest is provided in SM (Fig. A5).

2.6. Statistical analysis

Descriptive statistics (mean, median, standard deviation, maximum and minimum) were used to characterise the Sentinel-2 derived turbidity for each of the 8 tidal stages. Additionally, the difference of turbidity means of each tidal group was tested using a one-way ANOVA, and a post-hoc Tukey-Kramer test was applied to evaluate which pairs of means are statistically different.

To assess the impact of the tidal aliasing on long-term monitoring using a Sun-synchronous satellite, the monthly means for the six-year period, referred as annual climatologies in this manuscript, were generated over the 6 years period (2017–2022) of available data. Temporal analyses were performed on: 1) all-data monthly averaged Sentinel-2 -derived turbidity, as usually performed in remote sensing analyses, and 2) by dividing the images per-tidal-phase and performing separate time-series for the different tidal phases. A Wilcoxon Signed Rank test was used to evaluate if there are differences between the annual climatology of all-data turbidity and per-tidal-phase turbidity observed by a Sun-synchronous satellite. The coefficient of variation expressed as percentage (CV%) of the Sentinel-2 derived turbidity was employed to analyse the differences in tidal and seasonal variabilities.

3. Results

3.1. Turbidity algorithm performance

Match-up results of the calibrated Dogliotti et al. (2015) algorithm applied to MSI data showed a higher correlation with in situ measurements compared to the original algorithm, especially for turbidity values above 10 NTU (Fig. 3). The estimated turbidity with the calibrated method better aligns with the 1:1 line when compared with the original algorithm, which shows an underestimation of turbidity at higher concentrations.

3.2. Tidal sampling patterns in sun-synchronous satellites

To assess Sun-synchronous satellites to monitor tide-dominated systems, all available Sentinel-2 scenes for the period 2017–2022 were classified and labelled according to the tidal phase as explained in Fig. 2. Fig. 4 (left) shows that the number of Sentinel-2 scenes are not evenly distributed over the 8 tidal phases, with the flooding phase overrepresented compared to the ebbing phase, and low-tide is the most sampled tidal phase. Fig. 4 (right) shows that not all tidal condition are sampled by a Sun-synchronous satellite, especially in regards to the combination of spring/neap and semidiurnal cycles. High-tide phase is observed uniquely under weak neap tides and low-tide phase under weak spring tides. The highest tidal amplitudes (strongest spring tides at equinox period) are sampled exclusively during the first two Flooding phases (F1 and F2), while the lowest amplitudes (neap tides) are observed during the first ebbing phase. Overall, the flooding phases observed by Sentinel-2 are of higher tidal amplitude than the ebbing phases, which are observed uniquely under neap tides.

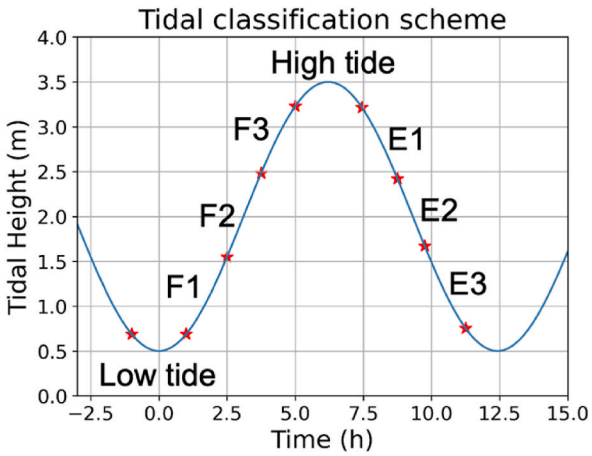

Fig. 2. Schematic representation of the semi-diurnal tidal stages used for the tidal classification.

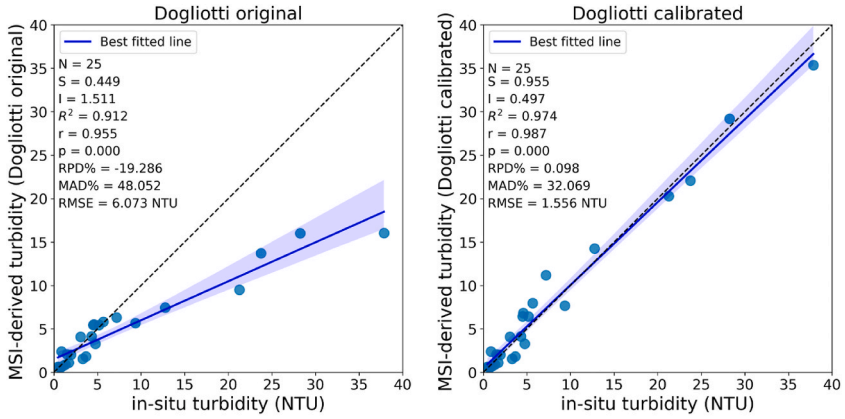

Fig. 3. Match-up results of original Dogliotti algorithm (left) and calibrated Dogliotti algorithm for the Tagus estuary (right).

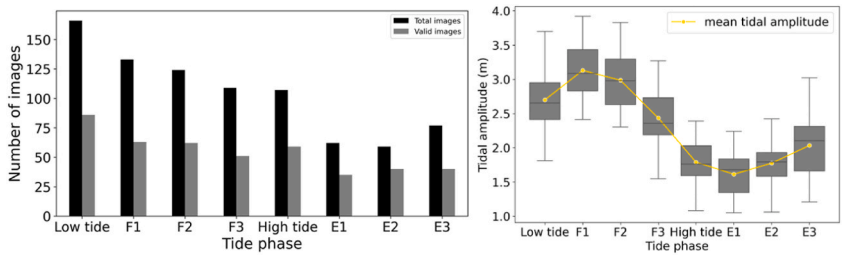

Fig. 4. Number of Sentinel-2 images distribution per tidal stage (left), and tidal amplitude observed for each of the 8 tidal stages (right). Valid images are the data that passed quality controls and used for the analysis of this work.

3.3. Tidal influence on satellite-derived turbidity

Fig. 5 shows the Sentinel-2 derived turbidity as a function of the semidiurnal and fortnightly tidal cycles. The highest turbidity concentrations are observed at the combination of spring tides with low water levels (LT, F1), while neap tides and high-tide phases are associated with low turbidity values, as expected. Fig. 5 (right) clearly illustrates the gradual variation in turbidity levels across the different tidal phases, aligning with the tidal variability expected for a tidal estuary, and thereby demonstrating the suitability of this classification method.

The fastest turbidity changes are shown at the final stage of both flooding and ebbing tides (F2 to F3 and E2 to E3), while the turbidity around the tidal peaks (both high and low) does not vary significantly, in accordance with the low tidal currents associated to these tidal phases. This is particularly relevant considering the differences in tidal amplitudes of the tidal phases observed around the tidal peaks, indicating that the semi-diurnal cycle also has a great impact in turbidity fluctuations. In fact, high turbidity values are also observed at E3, which present significantly lower amplitudes than LT and F1. Nonetheless, E2 presents lower turbidity than F2, associated with observations at lower tidal amplitude.

The one-way ANOVA test, confirms that there are statistically significant differences in turbidity of at least 2 tidal phases ($p <$

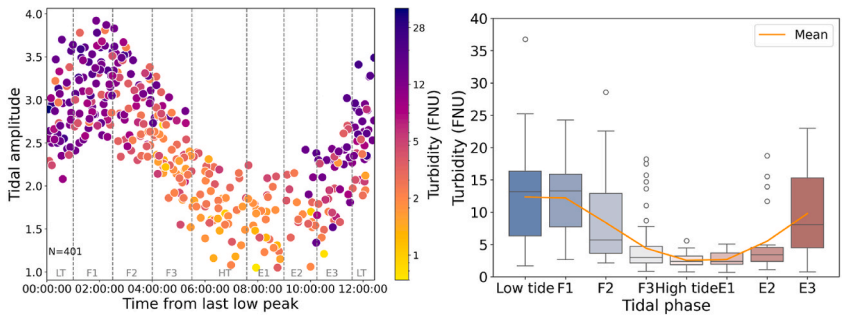

Fig. 5. Sentinel-2 derived turbidity against the Spring-Neap cycle (y-axis) and semidiurnal (x-axis) (left), and boxplot of Sentinel-2 -derived turbidity per tidal phase (right).

0.0001). Therefore a post-hoc Tukey's HSD test was performed to identify which specific pairs of tidal phases are significantly different. A graphical visualisation of Tukey's HSD test can be found in Fig. A1 of Supplementary Material. LT and HT are the pair with the greatest significant difference, as expected. The tide peaks and the following phase (HT-E1 and LT-F1) are the pairs with less significant differences. Comparing the tidal peaks (high- and low-tide), results suggest that water turbidity around high-tide peaks does not vary significantly, being F3, high-tide, E1 and E2 the tidal phases with less significant differences. Low-tide is significantly different from all other tidal phases except for F1.

3.4. Tidal impact on time-series analysis

To evaluate our Sentinel-2 tidal classification, we present here a spatio-temporal analysis of the turbidity product for the Tagus estuary. Given that no significant differences are observed between HT and E1, the two tidal phases were grouped in order to increase the number of available images, and will be referred, from now on, as high tide phase. Considering that low tide and F1 are the most sampled tidal phases, these two were not merged to ensure a similar number of images for the analysis of high tide and low tide (Fig. 4).

Fig. 6a–. c, and Fig. 6d illustrate the annual climatology of all data, low-tide, and high-tide data, respectively. The climatology of all tidal phases are provided in SM Fig. A2. We used the annual climatology of river discharge, corresponding to the same period of the Sentinel-2 data, as a proxy for seasonality of water turbidity, as we expect it to be the main driver of water turbidity. However, spring phytoplankton blooms and summer wind-driven bottom resuspension also play a major role in water turbidity in spring-summer months.

In Fig. 6, the similarity between low tide and all-data can be explained by the fact that low tide, being the most sampled tidal phase (Fig. 6b), is the most contributing tidal phase to the monthly turbidity value. All-data climatology present smaller annual variance compared to both low tide and high tide (Coefficient of Variation (CV) all data = 22.6%, CV LT = 29.0%, CV HT = 25.2%), due to the contribution of different tidal phases which smooth out the seasonal variability. As a result, any analysis of the temporal variability of turbidity based on all-data is biased by the contribution of different tidal conditions. Furthermore, the Wilcoxon test results suggest that all-data climatology is significantly different from all the per-tidal-phase filtered data climatologies ($p < 0.001$), except for the pair all-data - F2 ($p = 0.27$). It should be noted that the Wilcoxon test could not be performed on E2 and E3 tidal phases because some of the months had no data. Comparing the climatologies of the different tidal phases, the Wilcoxon test suggests that the climatologies of the groups around the tidal peaks are not significantly different from each other (full Wilcoxon results can be found in SM Table A1). The climatology of F2 is the most different from all other climatologies.

To further highlight the tidal impact on temporal analyses, the seasonal variability of turbidity of all-data and per-tidal phase filtered data at the entire estuary level is shown in Fig. 7. It can be noted that the turbidity variability across the estuary is consistently higher between tides than within tides, demonstrating the tidal impact on spatial gradients. Overall, tidal processes dominated over

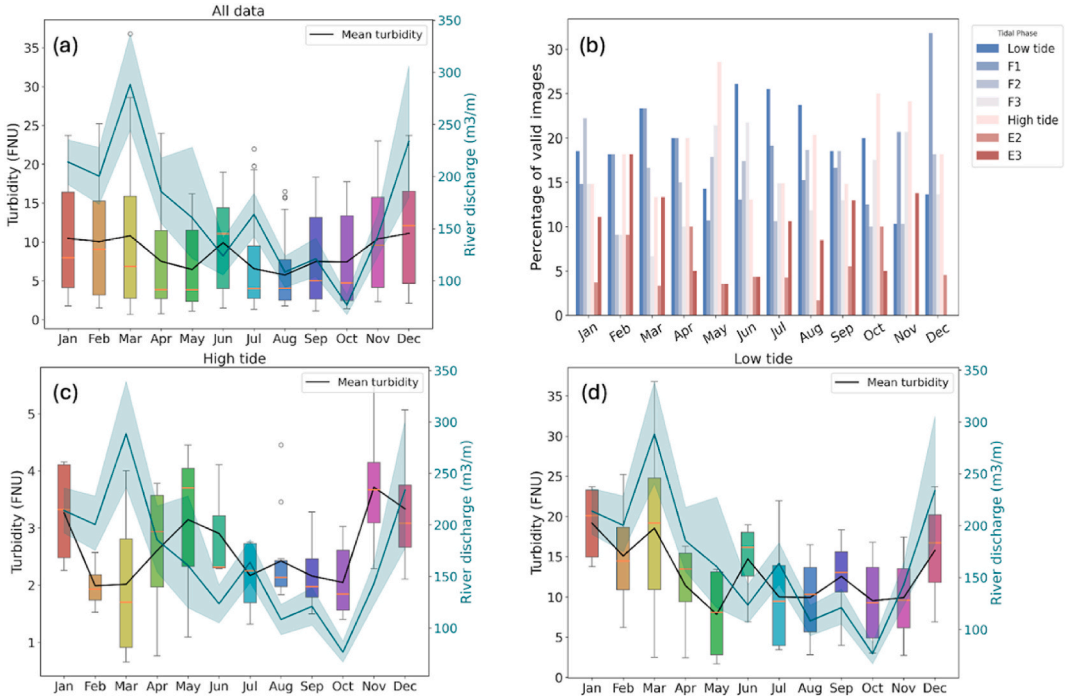

Fig. 6. Climatology of Sentinel-2 -derived turbidity of all-data (a), and per-tide-condition filtered data (Low tide (b) and High tide (c) (please note the different scales). The contribution of the different tidal phases to the total images used for the climatology of all data is shown in (b). Given that no significant differences were observed between High tide and E1, the two tidal phases were grouped to increase the number of valid images.

seasonal variability in the Tagus estuary, highlighting the importance of selecting a tidal condition when performing temporal analysis of water quality parameters in tidally dominated systems.

4. Discussion

4.1. Fluctuations given by different tidal conditions

In tidal estuaries, the temporal variation of water parameters is often primarily driven by tidal forces, reflecting the typical periodicities in tidal current speed and horizontal displacement of tidal waters (Blauw et al., 2012). These fluctuations can occur at different time-scales, from 6 h (semi-diurnal variability) to 15 days (spring-neap cycle). Our results show that a tidal classification of measurements taken at the same local solar time can clearly reveal the fluctuations given by different tidal conditions, showing a turbidity gradient expected for a tidal estuary. The statistical results indicate that the tidal phases around the tide peaks are not significantly different from each other, clearly indicating that low tidal currents are associated with small turbidity fluctuations.

Previous studies indicated that the spring-neap variation could be observed by remote sensing data, with higher concentration of SPM during Spring tides due to increased tidal currents and sediments resuspension (Valente and da Silva, 2009; Pietrzak et al., 2011). However, our results, which are in accordance with those of Eleveld et al. (2014) show that spring tides are always sampled at low-tide phases, which typically present higher levels of SPM or turbidity. Therefore, the high turbidity levels observed could be due to spring tides, low-tide phases or a combination of the two. From our results, the ebb phases present lower turbidity ranges than flooding stages, which is in contrast with the expected results for the Flood-dominated Tagus estuary. This is explained by the significantly lower tidal amplitudes associated with ebb images (neap tides, low tidal currents). All these results suggest that relying solely on remote sensing data for tidally-dominated systems can lead to misinterpretation of the spatio-temporal analysis of water quality parameters. As satellite images don't contain tidal phase information, additional data should be obtained to accurately analyse remote sensing observations of tidally-dominated systems.

4.2. Implications of sampling different tidal conditions

For this study, the Sentinel-2 satellites were selected as an example of a Sun-synchronous satellite, as they are frequently employed in transitional water studies given their higher spatial resolution. For the Tagus estuary, Sentinel-3 could also be adopted considering the wide basin that characterises the region, providing higher temporal revisit time and, therefore, higher chances of observing all possible tidal phases. However, we decided to focus on the Sentinel-2 as it is more frequently employed for transitional waters applications and similar results were obtained from tidal classification of Sentinel-3 (Figs. A3 and A4 in SM). In fact, at any locations, tides are not evenly distributed throughout the day, and even a satellite with daily revisit time will never observe all possible tidal conditions.

In this work we demonstrated that a Sun-synchronous satellite is not capable of observing all possible tidal phases in an estuary dominated by semidiurnal tides, and among the observed tidal conditions, some are over-sampled compared to others. This result is

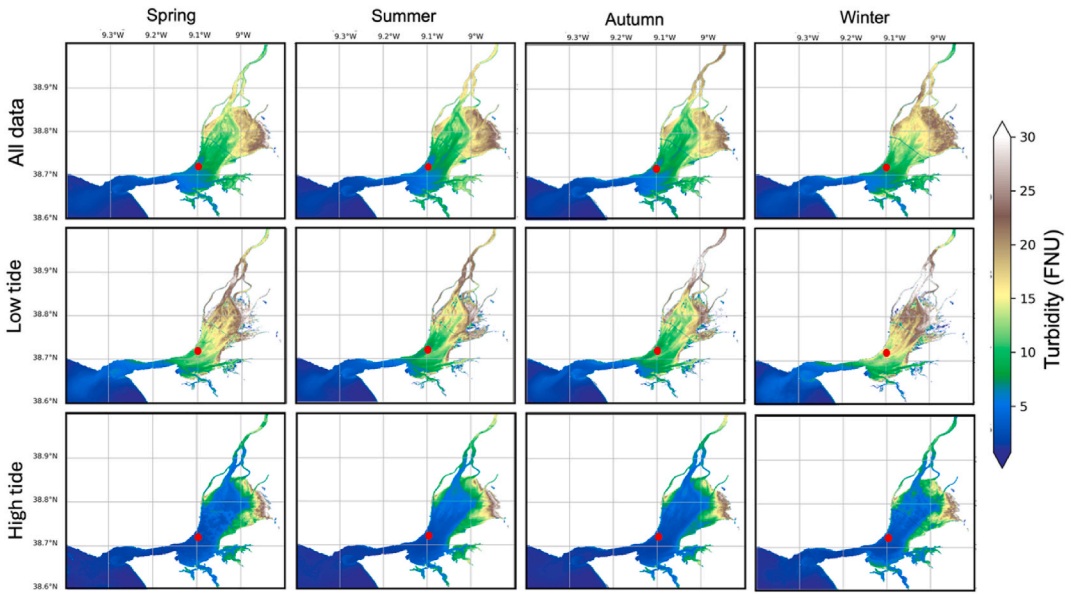

Fig. 7. Seasonal averages of the turbidity product for all-data, Low tide and High tide for the period 2017–2022. The red dot indicates the location of the polygon used for the analyses. Please refer to Fig. 1 for the detailed map of the study region. Please note that no bottom corrections were applied to the images.

aligned with previous studies (Valente and da Silva, 2009; Eleveld et al., 2014). Nevertheless, not enough importance has been given to these findings as most of the recent remote sensing applications to transitional systems do not account for the tidal effect when interpreting water quality changes over time. With the increasing number of remote sensing applications to transitional waters, the implication of tidal aliasing should be further highlighted. The uneven observation of tidal phases, with some being oversampled compared to others and some not observed at all, is particularly relevant if we consider all the emerging methods that use remote sensing data for data assimilation or as input source for algorithms training (e. g. machine learning or other types of Artificial Intelligence). In these methods, the representativeness of the training dataset plays a crucial role in the performance and general application of the algorithms. If the training is predominantly based on remote sensing data collected during specific tidal phases, the algorithms may struggle in the successful application to the less observed conditions. Additionally, this uneven sampling makes models developed from remote sensing data not truly comparable with models developed from in situ data.

Similarly, Optical Water Types (OWT) classification is becoming a popular tool for analysing the variability and trends of biogeochemical variables (Jackson et al., 2017; Spyrakos et al., 2018; Botha et al., 2020) and is often trained with remote sensing data. Here, the classification process can be distorted by the overrepresentation of certain tidal phases, and for instance, the resulting dominant OWT could reflect the most sampled tidal condition at satellite overpass time, but not necessarily be the dominant water type in the system. Therefore, it is essential to ensure that remote sensing data used for algorithms training or analysis adequately represent the full range of tidal phases observed within the study area, or at least be aware of the limitations of the method used.

4.3. Implications of tidal aliasing on water quality monitoring

Using satellite observations and tidal data, we show how tidal phase can affect the climatological analysis of turbidity in a mesotidal estuary. Analysis based on all-data versus per-tidal phase filtered data reveals significant differences, with all-data presenting lower interannual variability (CV all data = 22.6%, CV LT = 29.0%, CV HT = 25.2%). This discrepancy can be attributed to patchy and randomised observations due to meteorological conditions (i.e. cloud coverage). Some months may have more data from naturally high-turbidity tidal phases (e.g. low tide/spring tide), resulting in a higher monthly mean, not necessarily indicative of significant changes but only representative of the tidal phases observed. Several studies also highlighted the importance of the sampling intervals to properly capture the temporal variability of water parameters in transitional waters. For instance, Fettweis et al. (2023) compared water information obtained from sampling at different temporal resolutions and stated that infrequent or patchy samplings are not sufficient to properly capture temporal signals. Zhang et al. (2020) also noted that the relatively long-revisit time of Sun-synchronous satellites compared to the tidal cycle has limited their application to tidal flow studies and sediment dynamics. Additionally, Blauw et al. (2012) evaluated the influence of tidal cycles on chlorophyll and suspended sediments dynamics using continuous in situ data, concluding that irregular sampling intervals relative to natural tidal cycles can introduce biases in monitoring data. For example, sampling once daily at noon (typical scenario of ocean colour imagery), may inaccurately indicate water quality changes over several days, but reflecting the different tidal phases instead. The same authors also suggest that in systems dominated by semi-diurnal tides, measurements should have a fine temporal resolution (ideally hourly). Alternatively, sampling at consistent intervals relative to tidal cycles can help minimise the biases introduced by different tidal phases. This approach is frequently employed by in situ monitoring programs when continuous measurements from in situ sensors are not available. Our study intends to suggest that the same approach should be adopted also to remote sensing data.

Therefore, we recommend considering the tidal condition associated with each image when applying remote sensing data from a Sun-synchronous satellite to a tidally-dominated system. For coastal studies, we advise to use data acquired around the tidal peaks, where tidal currents are weaker and water parameters are stable within a longer time. This was further supported by our results that suggested that the water turbidity around the tidal peaks does not vary significantly, as a result of weak tidal currents around the high- and low-tides. In the context of water quality monitoring, we recommend the combination of low-tides at spring tides, as it should represent the worst possible scenario of water conditions, and in most cases should be the preferred tidal phase to be monitored. In terms of match-up analysis, our results indicate that the time window used for the match-ups in transitional systems could also vary depending on the tidal phase of satellite observation. The time-window commonly used in transitional systems is ± 1 h (Concha et al., 2021). However, we believe that this time could be extended if the satellite observation falls around the tidal peaks, when tidal currents are low. Cao and Tzortziou (2021) reported that, from field measurements of an estuarine system, the observed variability of water compositions within ± 3 h was typically exceeding the day-to-day variability at a similar tidal phase, and therefore, for match-ups with remote sensing data they used in situ data collected within ± 2 days, but only when the difference of tidal height between the satellite overpass and field measurement was less than 0.1 m. However, we argue that one should consider the tidal phase instead of the difference of tidal height, considering that the same tidal height can be observed under different conditions (i.e., during ebb or flood flows), which can translate into different water composition.

5. Conclusions

Remote sensing methods are becoming a tool widely applied for synoptic monitoring of a water system, frequently employed when there is interest in studying the temporal-spatial changes. However, in tidally-dominated systems there are tidal biases that need to be taken into consideration when an optical sensor mounted on a Sun-Synchronous satellite is used. Here, the tidal phase classification provided crucial insights into the water quality information retrieved by an Sun-synchronous satellite in a tidally-dominated system.

- Not all tidal phases are observed by a Sun-synchronous satellite, especially in regards to the combination of the spring/neap cycle and fortnightly cycles. Low-tide levels are uniquely observed under spring tides, high-tide levels are uniquely observed under neap tides, and the flood phases are observed at significantly higher tidal amplitudes than ebb phases; Spring low tides are over-represented compared to all other tidal conditions;
- the turbidity levels of the different tidal phases are significantly different from each others ($p < 0.0001$), highlighting the importance of performing time-series analysis on one single tidal phase;
- The time-series and climatology analysis provide significantly different results when considering all-data and per-tidal-phase filtered data ($p < 0.001$).

In conclusion, this work intendeds to alert the remote sensing community, and other users, about the critical importance of considering the tidal condition associated with each satellite overpass. Recognising these conditions is essential for improving the accuracy and applicability of remote sensing data to these environments.

CRediT authorship contribution statement

Giulia Sent: Writing – original draft, Methodology, Investigation, Formal analysis, Data curation, Conceptualization. **Carlos Antunes:** Writing – review & editing, Resources, Methodology. **Evangelos Spyrakos:** Writing – review & editing, Supervision, Methodology, Conceptualization. **Thomas Jackson:** Writing – review & editing, Supervision, Methodology. **Elizabeth C. Atwood:** Writing – review & editing, Resources, Methodology, Data curation. **Ana C. Brito:** Writing – review & editing, Supervision, Project administration, Methodology, Investigation.

Data availability

Data used in this work is publicly available at CERTO archive (https://engage.certo-project.org/data/). The tidal classification code is available in Github (https://github.com/giuliasent/TidalPhaseFinder).

Ethical statement

The authors declare that they followed all ethical practices in relation to the development, writing and publication of the article.

Declaration of competing interest

The authors declare that they have no known competing financial interests or personal relationships that could have appeared to influence the work reported in this paper.

Acknowledgements

This research was partially funded by the European Commission through the EU Horizon-2020 project CERTO (Copernicus Evolution - Research for harmonised and Transitional water Observation), grant number 870349. G.S. was funded by a PhD grant awarded by Fundação para a Ciência e a Tecnologia (FCT) within the scope of the MIT Portugal Program, grant number PRT/BD/153089/2021. A.C.B. was partially funded by FCT through the Scientific Employment Stimulus Programme (CEECIND/0095/2017). FCT also supported this study through the strategic projects (UID/MAR/04292/2020,LA/P/0069/2020) granted to MARE (https://doi.org/10.54499/UIDP/04292/2020) and ARNET ((//doi.org/10.54499/LA/P/0069/2020).

The authors wish to acknowledge the support of the wider CERTO consortium, who were essential to the completion of this study. The authors also sincerely acknowledge Bastian Raulier for the help in the initial design of the tidal classification code.

Appendix A. Supplementary data

Supplementary data to this article can be found online at https://doi.org/10.1016/j.rsase.2024.101425.

Data availability

Data will be made available on request.

References

Antunes, C., 2007. Previsão de Marés Portos principais de Portugal. FCUL Webpages. https://webpages.ciencias.ulisboa.pt/~cmantunes/hidrografia/hidro_mares.html.

APA, 2016. Parte 6_Anexos - Região hidrográfica do tejo e ribeiras do Oeste (rh5). https://doi.org/10.1179/1743132814Y.0000000460.

Barbier, E.B., Hacker, S.D., Kennedy, C., Koch, E.W., Stier, A.C., Silliman, B.R., 2011. The value of estuarine and coastal ecosystem services. Ecol. Monogr. 81 (2). https://doi.org/10.1890/10-1510.1.
Bettencourt, Alexandre, Bricker, Suzanne, Ferreira, J., Franco, A., Marques, João, Joanaz de Melo, João, Nobre, Ana, Ramos, Laddy, Reis, C., Salas, Fuensanta, Silva, Margarida, Simas, Teresa, Wolff, Wim, 2003. Typology and reference conditions for Portuguese transitional and coastal waters, development of guidelines for the application of the European union water Framework directive. TICOR. In: IMAR-INAG (Ed.). Lisbon, Portugal.
Bierman, P., et al., 2011. A review of methods for analysing spatial and temporal patterns in coastal Water quality. Ecol. Indicat. 11 (1). https://doi.org/10.1016/j.ecolind.2009.11.001.
Blauw, A.N., et al., 2012. Dancing with the tides: fluctuations of coastal phytoplankton orchestrated by different oscillatory modes of the tidal cycle. PLoS One 7 (11). https://doi.org/10.1371/journal.pone.0049319.
Botha, E.J., Anstee, J.M., Sagar, S., Lehmann, E., Medeiros, T.A.G., 2020. Classification of Australian waterbodies across a wide range of optical water types. Rem. Sens. 12 (18). https://doi.org/10.3390/RS12183018.
Braga, F., Scarpa, G.M., Brando, V.E., Manfè, G., Zaggia, L., 2020. COVID-19 lockdown measures reveal human impact on water transparency in the Venice Lagoon. Sci. Total Environ. 736. https://doi.org/10.1016/j.scitotenv.2020.139612.
Cao, F., Tzortziou, M., 2021. Capturing dissolved organic carbon dynamics with Landsat-8 and Sentinel-2 in tidally influenced wetland–estuarine systems. Sci. Total Environ. 777, 145910. https://doi.org/10.1016/j.scitotenv.2021.145910.
Cao, F., Tzortziou, M., 2024. Impacts of hydrology and extreme events on dissolved organic carbon dynamics in a heavily urbanized estuary and its major tributaries: a view from space. J. Geophys. Res.: Biogeosciences 129 (3). https://doi.org/10.1029/2023JG007767.
Catts, G.P., et al., 1985. Remote sensing of tidal chlorophyll-a variations in estuaries. Int. J. Rem. Sens. 6 (11), 1685–1706. https://doi.org/10.1080/01431168508948318.
Cereja, R., Chainho, P., Brotas, V., Cruz, J.P.C., Sent, G., Rodrigues, M., Carvalho, F., Cabral, S., Brito, A.C., 2022. Spatial variability of physicochemical parameters and phytoplankton at the Tagus estuary (Portugal). Sustain. Times 14 (20). https://doi.org/10.3390/su142013324.
Chen, J., et al., 2020. Monitoring dissolved organic carbon by combining landsat-8 and sentinel-2 satellites: case study in saginaw river estuary, lake huron. Sci. Total Environ. 718. https://doi.org/10.1016/j.scitotenv.2020.137374.
Concha, J.A., Bracaglia, M., Brando, V.E., 2021. Assessing the influence of different validation protocols on Ocean Colour match-up analyses. Rem. Sens. Environ. 259. https://doi.org/10.1016/j.rse.2021.112415.
Dias, J.M., Valentim, J.M., 2013. Numerical modelling of Tagus estuary tidal dynamics. J. Coast Res.
Dogliotti, A.I., et al., 2015. A single algorithm to retrieve turbidity from remotely-sensed data in all coastal and estuarine waters. Rem. Sens. Environ. 156, 157–168. https://doi.org/10.1016/j.rse.2014.09.020.
Doxaran, D., Froidefond, J.M., Castaing, P., Babin, M., 2009. Dynamics of the turbidity maximum zone in a macrotidal estuary (the Gironde, France): observations from field and MODIS satellite data. Estuar. Coast Shelf Sci. 81 (3), 321–332. https://doi.org/10.1016/j.ecss.2008.11.013.
Eleveld, M.A., van der Wal, D., van Kessel, T., 2014. Estuarine suspended particulate matter concentrations from sun-synchronous satellite remote sensing: tidal and meteorological effects and biases. Rem. Sens. Environ. 143, 204–215. https://doi.org/10.1016/j.rse.2013.12.019.
European Commission, 2003. Common Implementation Strategy for the Water Framework Directive (2000/60/EC). Guidance Document No. 5. Transitional and Coastal Waters - Typology, Reference Conditions and Classification Systems. Official J. European Union. http://www.waterframeworkdirective.wdd.moa.gov.cy/guidance.html.
Fettweis, M., et al., 2023. Sample based water quality monitoring of coastal seas: how significant is the information loss in patchy time series compared to continuous ones? Sci. Total Environ. 873. https://doi.org/10.1016/j.scitotenv.2023.162273.
Fortunato, A.B., Baptista, A.M., Luettich, R.A., 1997. A three-dimensional model of tidal currents in the mouth of the Tagus estuary. Continent. Shelf Res. 17 (14), 1689–1714. https://doi.org/10.1016/S0278-4343(97)00047-2.
Fortunato, A.B., Oliveira, A., 2005. Influence of intertidal flats on tidal asymmetry. J. Coast Res. 21 (5), 1062–1067. https://doi.org/10.2112/03-0089.1.
Fortunato, A.B., Oliveira, A., Baptista, A.M., 1999. On the effect of tidal flats on the hydrodynamics of the Tagus estuary. Oceanol. Acta 22 (1), 31–44. https://doi.org/10.1016/S0399-1784(99)80030-9.
Gameiro, C., Cartaxana, P., Brotas, V., 2007. Environmental drivers of phytoplankton distribution and composition in Tagus Estuary, Portugal. Estuar. Coast Shelf Sci. 75 (1–2), 21–34. https://doi.org/10.1016/j.ecss.2007.05.014.
Hudson, A.S., Talke, S.A., Jay, D.A., 2017. Using satellite observations to characterize the response of estuarine turbidity maxima to external forcing. Estuar. Coast 40 (2). https://doi.org/10.1007/s12237-016-0164-3.
Jackson, T., Sathyendranath, S., Mélin, F., 2017. An improved optical classification scheme for the Ocean Colour Essential Climate Variable and its applications. Rem. Sens. Environ. 203, 152–161. https://doi.org/10.1016/j.rse.2017.03.036.
Jiang, S., Xu, N., Li, Z., Huang, C., 2021. Satellite derived coastal reclamation expansion in China since the 21st century. Glob. Ecolog. Conserv. 30. https://doi.org/10.1016/j.gecco.2021.e01797.
Kennish, M.J., 2002. Environmental threats and environmental future of estuaries. Environ. Conserv. 29 (1), 78–107. https://doi.org/10.1017/S0376892902000061.
Masoud, A.A., 2022. On the retrieval of the water quality parameters from sentinel-3/2 and landsat-8 OLI in the nile delta's coastal and inland waters. Water 14 (4). https://doi.org/10.3390/w14040593.
Nascimento, Â., Biguino, B., Borges, C., Cereja, R., Cruz, J.P.C., Sousa, F., Dias, J., Brotas, V., Palma, C., Brito, A.C., 2021. Tidal variability of water quality parameters in a mesotidal estuary (Sado Estuary, Portugal). Sci. Rep. 11 (1). https://doi.org/10.1038/s41598-021-02603-6.
Neves, F.J.R.C., dos, S. da S., 2010. Dynamics and hydrology of the Tagus Estuary: results from "in situ" observations. PhD thesis, Universidade de Lisboa) 240. http://repositorio.ul.pt/handle/10451/2003.
Normandin, C., et al., 2019. Analysis of suspended sediment variability in a large highly turbid estuary using a 5-year-long remotely sensed data archive at high resolution. J. Geophys. Res.: Oceans 124 (11), 7661–7682. https://doi.org/10.1029/2019JC015417.
Oiry, S., Barillé, L., 2021. Using sentinel-2 satellite imagery to develop microphytobenthos-based water quality indices in estuaries. Ecol. Indicat. 121. https://doi.org/10.1016/j.ecolind.2020.107184.
Pahlevan, N., et al., 2022. Simultaneous retrieval of selected optical water quality indicators from Landsat-8, Sentinel-2, and Sentinel-3. Rem. Sens. Environ. 270. https://doi.org/10.1016/j.rse.2021.112860.
Pendleton, Linwood H., 2011. The Economic and Market Value of Coasts and Estuaries: What's at Stake? Restore America's Estuaries, Arlington, VA, USA.
Pietrzak, J.D., de Boer, G.J., Eleveld, M.A., 2011. Mechanisms controlling the intra-annual mesoscale variability of SST and SPM in the southern North Sea. Continent. Shelf Res. 31 (6), 594–610. https://doi.org/10.1016/j.csr.2010.12.014.
Sent, G., Biguino, B., Favareto, L., Cruz, J., Carolina, S., In, A., Palma, C., Brotas, V., Brito, A.C., 2021. Deriving water quality parameters using sentinel-2 imagery : a case study in the sado estuary , Portugal. Rem. Sens. 13, 1043. https://doi.org/10.3390/rs13051043.
Sent, G., 2020. Remote sensing for water quality studies : test of Suspended Particulate Matter and turbidity algorithms for Portuguese transitional and inland waters (MSc dissertation, Universidade de Lisboa, Faculdade de Ciências). https://repositorio.ul.pt/handle/10451/45463.
Spyrakos, E., O'Donnell, R., Hunter, P.D., Miller, C., Scott, M., Simis, S.G.H., Neil, C., Barbosa, C.C.F., Binding, C.E., Bradt, S., Bresciani, M., Dall'Olmo, G., Giardino, C., Gitelson, A.A., Kutser, T., Li, L., Matsushita, B., Martinez-Vicente, V., Matthews, M.W., Tyler, A.N., 2018. Optical types of inland and coastal waters. Limnol. Oceanogr. 63 (2), 846–870. https://doi.org/10.1002/lno.10674.
Steinmetz, F., Deschamps, P., Ramon, D., 2011. Atmospheric correction in presence of sun glint: application to MERIS. Opt Express 19, 9783–9800. https://doi.org/10.1364/oe.19.009783.
Stelzer, K., et al., 2020. Copernicus Global Land Operations 'Cryosphere and Water' 'CGLOPS-2 - Lot 2'.
Tao, J., Hill, P.S., 2019. Correlation of remotely sensed surface reflectance with forcing variables in six different estuaries. J. Geophys. Res.: Oceans 124 (12). https://doi.org/10.1029/2019JC015336.

Valente, A.S., da Silva, J.C.B.B., 2009. On the observability of the fortnightly cycle of the Tagus estuary turbid plume using MODIS ocean colour images. J. Mar. Syst. https://doi.org/10.1016/j.jmarsys.2008.08.008.

Vaz, N., Mateus, M., Dias, J.M., 2011. Semidiurnal and spring-neap variations in the Tagus estuary: application of a process-oriented hydro-biogeochemical model. J. Coast Res. 1619–1623.

Wang, S., Shen, M., Ma, Y., Chen, G., You, Y., Liu, W., 2019. Application of remote sensing to identify and monitor seasonal and interannual changes of water turbidity in yellow river estuary, China. J. Geophys. Res.: Oceans 124 (7). https://doi.org/10.1029/2019JC015106.

Yang, C., Ye, H., Tang, S., 2020. Seasonal variability of diffuse attenuation coefficient in the Pearl river estuary from long-term remote sensing imagery. Rem. Sens. 12 (14). https://doi.org/10.3390/rs12142269.

Zhai, T., Wang, J., Fang, Y., Qin, Y., Huang, L., Chen, Y., 2020. Assessing ecological risks caused by human activities in rapid urbanization coastal areas: towards an integrated approach to determining key areas of terrestrial-oceanic ecosystems preservation and restoration. Sci. Total Environ. 708. https://doi.org/10.1016/j.scitotenv.2019.135153.

Zhang, X., Fichot, C.G., Baracco, C., Guo, R., Neugebauer, S., Bengtsson, Z., Ganju, N., Fagherazzi, S., 2020. Determining the drivers of suspended sediment dynamics in tidal marsh-influenced estuaries using high-resolution ocean color remote sensing. Rem. Sens. Environ. 240 (January), 111682. https://doi.org/10.1016/j.rse.2020.111682.